**Article:**
Smith, P. orcid.org/0000-0003-3001-0245, McLauchlin, A., Franklin, T. orcid.org/0000-0002-5152-6235 et al. (8 more authors) (2024) A data-driven analysis of HDPE post-consumer recyclate for sustainable bottle packaging. Resources, Conservation and Recycling, 205. 107538. ISSN 0921-3449

https://doi.org/10.1016/j.resconrec.2024.107538

Resources, Conservation & Recycling 205 (2024) 107538

Contents lists available at ScienceDirect

Resources, Conservation & Recycling

journal homepage: www.elsevier.com/locate/resconrec

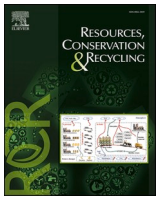

Full length article

# A data-driven analysis of HDPE post-consumer recyclate for sustainable bottle packaging

Philip Smith [a], Andy McLauchlin [b,f], Tom Franklin [b,f], Peiyao Yan [c], Emily Cunliffe [c], Tom Hasell [c], Vitaliy Kurlin [a], Colin Kerr [d], Jonathan Attwood [e], Michael P. Shaver [b,f], Tom O. McDonald [b,f,*]

[a] Department of Computer Science, University of Liverpool, Liverpool L69 3DR, UK
[b] Henry Royce Institute, The University of Manchester, Oxford Road, Manchester, M13 9PL, UK
[c] Department of Chemistry, School of Physical Sciences, University of Liverpool, L69 7ZD, UK
[d] Unilever Research and Development, Port Sunlight, Birkenhead CH62 4UY, UK
[e] IPL Brightgreen, Newton Ln, Allerton Bywater, Castleford WF10 2AL, UK
[f] Department of Materials, The University of Manchester, Oxford Road, Manchester, M13 9PL, UK

ARTICLE INFO

*Keywords:*
Post-consumer recyclate (PCR)
Plastics recycling
High-density polyethylene
Datadriven analysis
Polymer characterization
Circular economy

ABSTRACT

The packaging industry faces mounting demand to integrate post-consumer recyclate (PCR). However, the complex structure-property relationships of PCRs often obscure their performance compared to virgin equivalents, posing challenges in selecting suitable PCRs for applications. Focused on extrusion blow moulding grade high-density polyethylene (HDPE), this study presents the most extensive characterisation of HDPE PCR to date, encompassing 23 resins (3 virgin, 20 PCR). Employing Fourier-transform infrared spectroscopy (FTIR), differential scanning calorimetry (DSC), thermogravimetric analysis (TGA), rheology, colour analysis, and mechanical testing, we established a feature-rich dataset with 56 distinctive characteristics. Utilising a data science approach based on principal component analysis, with the virgin samples as a benchmark, we identified that combining FTIR, TGA and mechanical testing provided effective identification of PCRs that closely match the properties of virgin HDPE. The pipeline created can be utilised for new PCRs to determine suitability as a replacement for virgin plastic in a desired application.

## 1. Introduction

Plastics are materials that underpin modern life due to their versatility, sterility and low-cost. However, the low-cost and durability of plastics has led to significant environmental impact due to their disposal and persistence (McIlgorm et al., 2022). Additionally, without significant new policies to reduce demand and increase circularity,(OECD, 2022) the global demand for plastics is predicted to increase from 390.7 Mt in 2022 (PlasticEurope: Plastics – The Facts 2022, 2022) to 1231 Mt in 2060. The plastic pollution issue is compounded as the $CO_2$ production associated with the manufacturing of virgin plastics from fossil feedstocks is a considerable contributor to global emissions and needs to be reduced to support Net Zero targets (Zheng and Suh, 2019) A major application of plastics is in the packaging sector, which represents approximately 40% of total plastics use in Europe and is one of the sectors with the shortest usage lifetime (PlasticEurope: Plastics – The Facts 2022, 2022). However, plastics are an efficient material for packaging applications as replacing plastics with other materials has been shown to increase energy use and $CO_2$ production (Abejón et al., 2020; Silva and Molina-Besch, 2023; Tamburini et al., 2021). Therefore, the current strategy is to move from a linear use model towards a more circular use of plastics to reduce the environmental impact (Tenhunen-Lunkka et al., 2023). Within the UK, this opportunity has been supported by national targets, and taxes as well as increasing consumer demands have resulted in a drive to increase the use of post-consumer recyclate (PCR) in packaging products. That said, it is likely that new regulations and changes in demand and consumption will be required to meet the intended circular economy impacts (Lisiecki et al., 2023). Ultimately, barriers to increased recycling and PCR use need to be minimised to enhance the sustainability of plastics (Bachmann et al., 2023).

High-density polyethylene (HDPE), the second most widely used plastic in packaging applications in the UK after poly(ethylene

* Corresponding author at: Henry Royce Institute, The University of Manchester, Oxford Road, Manchester, M13 9PL, UK.
*E-mail address:* Thomas.McDonald@Manchester.ac.uk (T.O. McDonald).

https://doi.org/10.1016/j.resconrec.2024.107538
Received 5 December 2023; Received in revised form 6 February 2024; Accepted 1 March 2024
Available online 12 March 2024

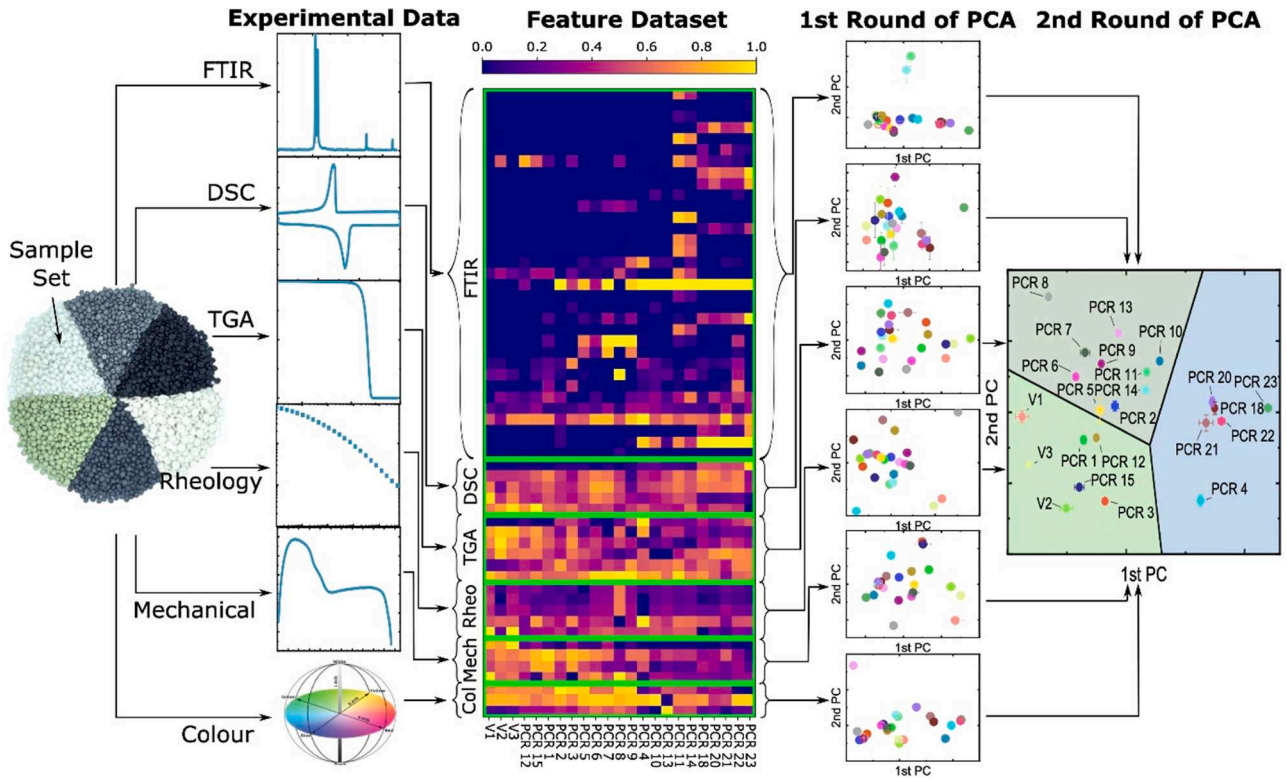


**Fig. 1.** An overview of the data science approach. Starting from our sample set of 23 HDPE resins (3 virgin, 20 PCR), we extract six sets of experimental data: FTIR, DSC, TGA, rheology, mechanical and colour. From here, we identify key features that form our feature dataset (centre). Performing PCA on the features of each experiment reveals how each technique distinguishes the resins. Taking the first two PCs of the PCAs of each experimental technique (12 features in total), we perform a second iteration of PCA. This gives us a visualisable description of how the resins compare with each other.

terephthalate) (Thomson et al., 2018). is widely collected in post-consumer recycling bins and offers significant potential for PCR utilisation (Hahladakis et al., 2018). HDPE is commonly employed in the manufacturing of bottles for both food and non-food applications due to its excellent strength, durability, and chemical resistance. However, the HDPE used in packaging comprises a diverse range of grades tailored to meet specific bottle requirements, resulting in variations in properties and performance. Additionally, polypropylene (PP) is typically used in the lids of HDPE bottles and possesses a similar density (895–920 kg/m$^3$) to HDPE (930–970 kg/m$^3$), leading to PP being a common contaminant of HDPE PCR along with volatiles, inks, labels, and other plastics in the waste stream (Van Belle et al., 2020). Bottle producers are also concerned about the odour and colour of PCR as this may affect consumer perception of the packaged product. Furthermore, the additional extrusion processes involved in mechanical recycling results in potential degradation through heat, shear, and oxidation (Schyns and Shaver, 2020). The resulting changes in the properties of the PCR present a significant challenge in determining the performance and suitability of PCR compared to virgin plastics (Akhras et al., 2023; Freudenthaler et al., 2022). The challenge of using PCR to replace virgin HDPE is exacerbated by the incomplete understanding of the structure-property relationships inherent in PCR materials. Therefore, thoroughly characterising HDPE PCR is crucial to gaining insights into its potential as a replacement for virgin HDPE in terms of its mechanical properties.

In the last few years there has been a considerable growth in the research investigating the properties of HDPE PCR. Gall et al. characterised in detail six HDPE PCRs from Austria and Germany and concluded that polyolefin contamination was common and tended to influence density and impact strength, whereas inorganic fillers such as calcium carbonate were present in amounts less likely to affect physical properties (Gall et al., 2021). Karaagac et al. showed that low amounts of PP drastically affected the tensile and impact properties of recycled HDPE but that blending with olefin block copolymer mitigated these effects (Karaagac et al., 2021b). Other researchers have found a similar negative effect caused by PP contamination in HDPE PCR, for example Akhras et al. found that manually sorted (informal) HDPE PCR from PET bottle caps had lower contamination than that sorted automatically at materials recycling facilities (Akhras et al., 2023). Freudenthaler et al. tested two PCRs as blends with virgin HDPE for potential applications in pipes; differences in contamination with PP and the presence of $CaCO_3$ between the two PCR materials were linked to the environmental stress cracking resistance (Freudenthaler et al., 2022). Mager et al. compared HDPE PCR from producers using automated sorting technologies with informal, hand-picking approaches to sorting and considered the substitution potential of PCRs based on the melt flow index, Young's modulus and Charpy impact strength (Mager et al., 2023). We have previously shown that PCR offers much poorer performance in terms of environmental stress cracking resistance in bottles than virgin HDPE. (McLauchlin et al., 2023). This inferior performance may limit the potential for PCR to be used in bottles containing cleaning products. Given the variability between PCR suppliers and even between batches (Benyathiar et al., 2022; Orzan et al., 2021). it is important to capture this variability by testing many different samples. The most informative approaches to date for determining differences in HDPE have been detected by Fourier-transform infrared spectroscopy (FTIR) (Camacho and Karlsson, 2002a; Gall et al., 2021). differential scanning calorimetry (DSC) (Camacho and Karlsson, 2001; Manivannan and Seehra, 1997). thermogravimetric analysis (TGA) (Achilias, 2022; Camacho and Karlsson, 2002b). rheology (Karaagac et al., 2021b; Oblak et al., 2015). environmental stress cracking resistanc (Kurelec et al., 2005; Van Beek and Deblieck, 2011). and mechanical testing (Alzerreca et al., 2015; Karaagac et al., 2021a). Typically, this data is analysed by a univariate approach, however this method is insufficient for identifying trends that

are driven by combinations of factors. One approach to assess the suitability of PCRs in given applications is the method shown by Demets et al (Demets et al., 2021). in which application specific functions focussed on processability and mechanical recycling quality were used to generate a score. This approach has subsequently been used to inform PCR selection for rigid packaging (Mager et al., 2023). and in non-packaging applications (Akhras et al., 2023). Another approach is principal component analysis (PCA), a powerful tool that can be used to reduce the dimensionality of the dataset whilst preserving the directions of the data that explain the most variation (Ringnér, 2008). As such, the principal components (PCs) are a good summary of the variations present within the dataset. An example is the work of da Silva and Wiebeck who applied PCA and partial least squares regression to FTIR data to determine the compositional fraction of HDPE/LDPE blends (da Silva and Wiebeck, 2022). There is a considerable opportunity to use data science tools such as PCA to process the complex, high-dimensional data produced by multiple characterisation methods of highly variable materials such as HDPE PCR.

In this study, we present the most extensive characterisation of HDPE PCR to date. Our investigation involves a sample set of 23 HDPE resins, comprising 20 HDPE PCRs and three virgin HDPEs. By encompassing a wide range of HDPE resins, we capture the heterogeneity arising from different sources, separation methods and recycling processes. After analysing the materials by FTIR, DSC, TGA, rheology, colour analysis and mechanical testing, we used a three-step data science process (Fig. 1) involving feature selection, identification of the most significant features by PCA, and a second iteration of PCA to compare the resins with each other. Finally, by utilising virgin HDPE samples as benchmarks, we quantified the performance of PCR and established correlations among the features extracted from our dataset. We are then able to highlight the subset of experimental techniques that offer the most informative results within limited time and resource constraints. The comprehensive dataset and the insights derived from our study offer a valuable resource for the packaging industry and researchers alike. By leveraging our method of analysis, future assessments of new PCR materials can be expedited, enabling the identification of suitable replacements for virgin plastics in specific applications.

## 2. Materials

Three virgin HDPEs of extrusion blow moulding grade were included in this study. They are LyondellBasell's Hostalen 5231 D (V1), Chevron Phillips Chemical's Marlex HHM 5502BN (V2), and LyondellBasell's Hostalen 5831D (V3).

The requirements for selection of the HDPE PCR samples for inclusion in this analysis were that they were commercially available and listed as extrusion blow moulding grade. The melt flow index (MFI) of the PCRs obtained for this study were in the range 0.1 to 0.89 g/10 min (190 °C/2.16 kg) and therefore suitable for extrusion blow moulding. Once received, the PCR pellets were stored in sealed containers under ambient conditions. The specific names of the PCR samples are not given due to commercial considerations. The countries of origin included: The United States (2 resins); Netherlands (8 resins); Italy (2 resins); Spain (1 resin); Poland (4 resins) and the United Kingdom (6 resins).

## 3. Methods

### 3.1. FTIR

Mid-infrared spectra of all samples were recorded on a Vertex 70 FTIR Spectrometer (Bruker Instruments, Coventry, UK) in attenuated total reflectance mode (ATR) on cut surfaces of pellets. 32 scans for each sample were collected over a scan range of 4000–600 $cm^{-1}$ at a resolution of 2 $cm^{-1}$, and were normalised so that the highest peak had an absorbance of 1.

A minimum threshold was necessary to remove from consideration features of the FTIR spectrum that are due to noise or negligible contaminates. A maximum threshold was necessary to ensure that where a strong feature was present for all resins this can be removed from consideration too since it does not distinguish the resins. With these thresholds, every feature of the FTIR spectrum is assigned a value from zero to one: a value of zero if the strength of the feature is below the minimum threshold; a value of one if the strength of the feature is above the maximum threshold; and a value between zero and one if the strength of the feature lies between the minimum and maximum thresholds (linearly computed). We then manually removed features that were due to carbon dioxide.

### 3.2. Thermal analysis

All thermal analysis was done on a TA Instruments (New Castle, DE, USA) Discovery differential scanning calorimeter. Specimens for analysis in triplicate (5 mg ± 0.5 mg) were either cut from individual pellets or weighed from cryomilled pellet as required and sealed in aluminium pans. To determine the melting point and enthalpies of fusion and crystallisation, specimens were equilibrated at 50 °C under a nitrogen atmosphere, heated to 200 °C, held isothermally for 3 min, cooled to 50 °C, held isothermally for 3 min and finally heated again to 200 °C in accordance with ASTM D3418-15 (ASTM International, 2012). The heating and cooling rates were 10 °C $min^{-1}$.

Some PCR samples contained polypropylene (PP) which gives an endothermic peak at 160 °C and the fraction of PP ($f_{PP}$) was calculated using Eq. (1)

$$f_{PP} = \frac{\frac{Normalised_{PP}}{\Delta H_{PP}}}{\left(\frac{Normalised_{PP}}{\Delta H_{PP}}\right) + \left(\frac{Normalised_{HDPE}}{\Delta H_{HDPE}}\right)} \quad (1)$$

where

- $\Delta H_{PP}$= Enthalpy of crystallisation of PP (208 $J/g$);
- $\Delta H_{HDPE}$= Enthalpy of crystallisation of HDPE (293 $J/g$);
- $Normalised_{PP}$= Normalised peak area of PP peak;
- $Normalised_{HDPE}$= Normalised peak area of HDPE peak.

The true normalised HDPE was then calculated by Eq. (2)

$$TrueNormalised_{HDPE} = \frac{Normalised_{HDPE}}{1 - f_{PP}} \quad (2)$$

and the crystallinity of the HDPE was then calculated by Eq. (3)

$$\%\ Crystallinity = 100\ \times \frac{TrueNormalised_{HDPE}}{\Delta H_{HDPE}} \quad (3)$$

Thermogravimetric analysis (TGA) was performed using a Q5000IR analyser (TA Instruments, New Castle, DE, USA) with an automated vertical overhead thermobalance, by heating duplicate 5 mg ± 0.5 mg samples in platinum crucibles under nitrogen over the range 40 °C to 600 °C at a heating rate of 10 °C $min^{-1}$.

### 3.3. Colour analysis

The colour of each sample was recorded on a Konica Minolta 2600d (Warrington, UK), with a built-in light source, using the L*a*b* colour scale. Five replicate measurements were made on individual subsamples of pellets contained in a Petri dish.

### 3.4. Mechanical analysis

For measurement of tensile properties, sheets of nominal thickness 4 mm were pressed at 5 MPa pressure for 20 min at 180 °C and cooled over 60 min to 40 °C. Sheets of thickness 1 mm for the strain hardening modulus (SHM) measurement were prepared by compression moulding

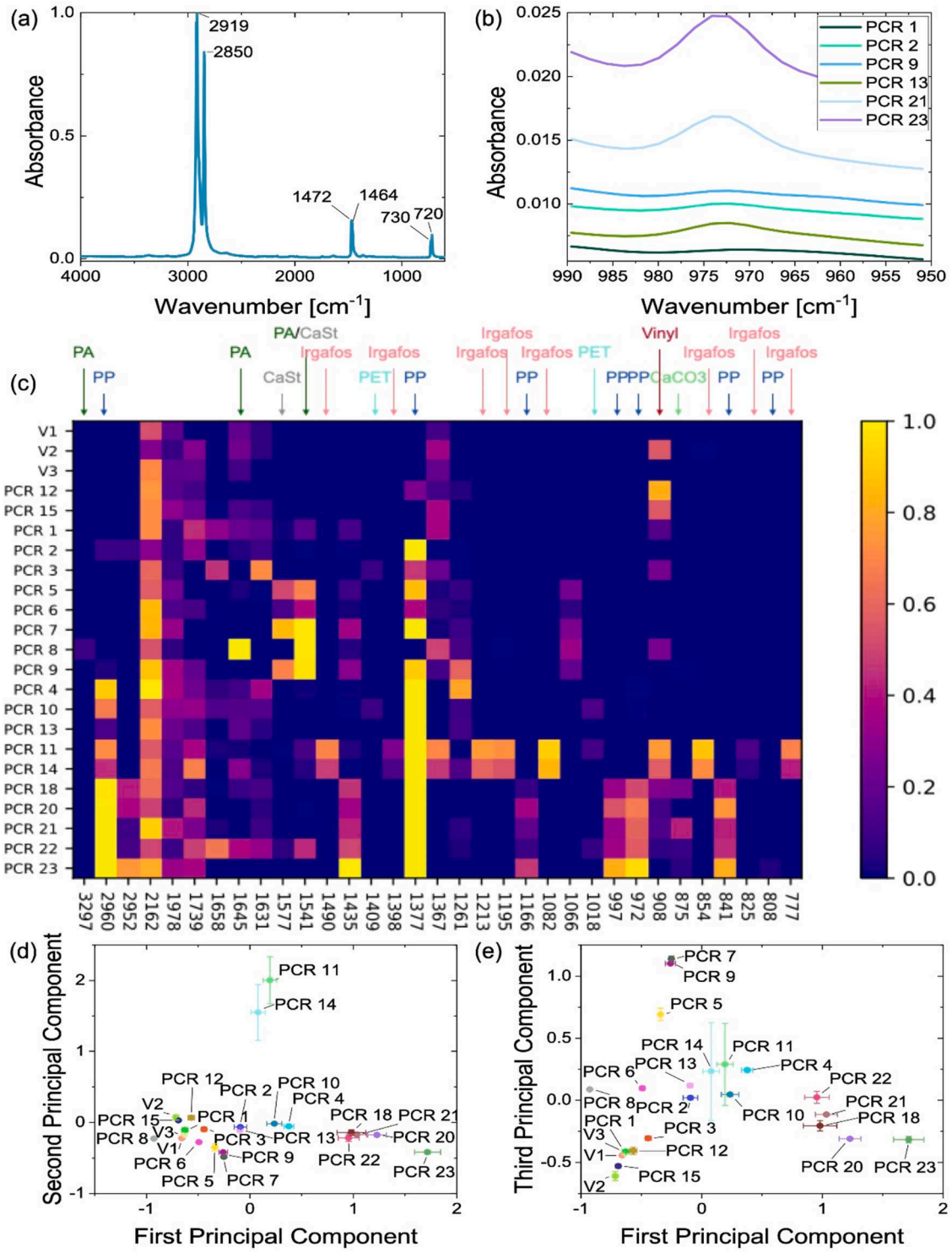


**Fig. 2.** Using a data science approach with FTIR data to distinguish the PCR samples. a) A standard FTIR spectrum for virgin HDPE (LyondellBasell's Hostalen ACP 5231 D). All resins in our sample set, whether virgin or PCR, contained these six characteristic peaks of HDPE in their spectra. b) A closer look shows that FTIR distinguishes resins for minor peaks that do not correspond to HDPE. For example, this snippet from wavenumbers 990 to 950 $cm^{-1}$ shows a peak that corresponds to PP that is present in some but not all the resins. c) An FTIR heat map for the resins. This plot is produced automatically and can be used to identify potential contaminants of the resins. d) The first PC of the PCA of the FTIR features against the second PC. e) The first PC against the third PC.

according to ISO 923/ISO 17,855–2. (ISO, 2016). For measurement of the SHM, test specimens with gauge length 12.5 mm were prepared by compression moulding according to ISO 923/ISO 17,855–2 followed by annealing for 60 min at 120 °C and allowed to cool in the oven overnight.

Tensile properties of the blends were tested according to ISO527 (ISO, 2012). after conditioning at 23 °C and 50% relative humidity. Measurement of the SHM was performed according to BS ISO 18488:2015 (ISO, 2015). using an environmental chamber (Severn Thermal Solutions, Dursley, UK) to maintain the testing temperature of 80 °C.

All tensile and SHM tests were done using an Instron TM-340 testing

frame with 10 kN load cell (Instron, High Wycombe, UK). Five replicate tests were done for SHM and seven specimens from each PCR were tested for tensile properties. The testing speeds for tensile properties and SHM were 50 mm $min^{-1}$ and 20 mm $min^{-1}$, respectively. Data was processed using Bluehill Universal software (Instron, High Wycombe, UK).

### 3.5. Rheological analysis

Rheological analysis was done in oscillatory mode at 190 °C using a MCR320 Rheometer (Anton Paar Instruments, Graz, Austria) using a parallel plate geometry. Duplicate frequency sweeps were run at 5% strain, chosen after a preliminary amplitude sweep to verify that this was in the linear viscoelastic region (see Fig. S1), over the range 500–0.01 rad $s^{-1}$. Data was processed using Rheocompass™ software (Anton Paar Instruments, Graz, Austria).

### 3.6. Data analysis

#### 3.6.1. PCA

The PCA of the feature dataset was performed in Python using scikit-learn's PCA implementation. PCA was first applied to the features of each of the six experimental techniques to reduce the number of features for each technique to two by taking the first two PCs of the PCA. Hence the reduced feature dataset is 12-dimensional. We applied a second iteration of PCA to this 12-dimensional dataset, and the first two PCs are those plotted in Fig. 5.

#### 3.6.2. Identifying most significant triplet of techniques

We can use the two-dimensional space obtained in our overall PCA analysis (Fig. 5). to define a distance to virgin for a PCR. Namely, for a given PCR, we compute in this two-dimensional space the Euclidean distance between the PCR and each of the three virgin resins, and then take the mean. We define this value to be the ground truth mean distance of a PCR resin to virgin HDPE.

We define the significance of a subset of experiments to be how well the subset preserves the ground truth mean distances of the PCRs when the subset is put through the same pipeline. Namely, for the given subset, as before, PCA is applied to the features of each of the experimental techniques in the subset to reduce the number of features of each technique to two, namely the first two PCs. We combine the two features of each technique to form a 2n-dimensional dataset, where n is the number of techniques in the subset. We apply PCA to this 2n-dimensional dataset and take the first two PCs to form a two-dimensional space. Then, as before, for each resin, we compute the Euclidean distance of the resin from each of the virgin resins and take the mean. This gives us the mean distance of the PCR to virgin HDPE for this subset of experiments. For each PCR, we then take the absolute value of the difference between its mean distance to virgin HDPE for this subset and its ground truth mean distance to virgin HDPE, thus quantifying how much this triplet of experiments preserves the ground truth distance for this PCR. Taking the mean of these differences across all the PCRs gives us our final value for a subset. For example, if our subset is actually all six experimental techniques, the mean difference will be zero. A subset of techniques with a mean difference from the ground truth of 0.5 means that on average the mean distance between a PCR and virgin HDPE as computed using the subset of techniques differs by 0.5 compared to the ground truth mean distance of that PCR to virgin HDPE. When we focus on triplets of experiments, FTIR, TGA and mechanical techniques is the best triplet with a mean difference of 0.2 (Fig. 6)..

## 4. Results and discussion

Six experimental techniques were used to extract data from each of the 23 resins in our sample set. Specifically, we performed: FTIR: characterises the functional groups present in the sample; DSC: reveals the crystallinity of the sample; TGA: sheds light on the purity and composition of the sample; Rheology: measures the viscosity and shear thinning behaviour of the polymer melt; Mechanical: determines tensile properties and also the strain hardening modulus, which has been shown for virgin HDPE to be predictive of the environmental stress cracking resistance (Kurelec et al., 2005). We also measured the colour of each sample which provides some insights into the source of the materials used to create the PCR. For instance, it may suggest that colour sorting has been carried out which may reduce the complexity of the feedstock. One challenge with attempting to distinguish HDPE resins is that many characteristics and properties show variability within samples, with greater variability expected for PCRs. Therefore, the majority of measurements were carried out with at least 3 replicates to identify intra-batch variability as well as experimental noise. Given the scale of the data obtained from the combined analysis methods, this paper will focus on the three analysis methods that were identified to be the most significant for differentiating the PCRs – FTIR, TGA and mechanical testing. (How this triplet was identified to be the most significant is discussed later in the paper.) A second paper will discuss the relationships between the other characterisation methods.

From the analysis of the 23 HDPE samples, 56 features were extracted from the data obtained from the six characterisation methods performed. A breakdown of these features can be seen in Table S2 in the supplementary information. These features formed our feature dataset, with each feature normalised so that its range is from zero to one (see centre of Fig. 1).. This feature dataset is then used as the input of further analysis techniques. We will exemplify this feature selection with the FTIR data.

### 4.1. Approach to feature selection, exemplified with FTIR data

The FTIR spectra of the resins show that the typical peaks for polyethylene were present for all samples. These occur at wavenumbers 2919, 2850, 1472, 1464, 730, and 720 $cm^{-1}$ (Fig. 2a) (Noda et al., 2007). However, minor peaks that originate from additives and contaminates can be used to differentiate samples (Gall et al., 2021; Mager et al., 2023). For example, at 972 $cm^{-1}$ a peak can be assigned to $CH_3$ rocking in PP which is only detected in a selection of the samples (Fig. 2b) (Campanale et al., 2023; Noda et al., 2007). To enable the identification of subtle differences between samples we used the second and third derivatives of the FTIR spectrum to automatically identify a total of 33 features. A feature was identified to be the wavenumber at which the third derivative passes through zero from negative to positive. The benefit of this approach was that, in addition to peaks, shoulders of peaks could be automatically detected too. We define the strength of a feature for a given specimen to be the absolute amplitude of the second derivative at this wavenumber, effectively capturing how sharp the peak or shoulder is (see Fig. S3 in the SI for a visualisation of this approach). We defined manually minimum and maximum thresholds for the strength of the features (discussed in the methods section) to remove features due to noise and dominant features present in all specimens (i.e., features due to HDPE) and then we normalised each feature. We can visualise this data for all resins in Fig. 2c.

An analysis of this plot has been used to identify additives and contaminates of the resins. For example, wavenumbers 2960, 1377, 1166, 997, 972 and 841 $cm^{-1}$ all correspond to PP contaminate (Noda et al., 2007). and across these wavenumbers we see that PCRs 18, 20, 21, 22 and 23 regularly have the highest values, suggesting that these are the resins most contaminated with PP. Some level of PP contamination was detected in most PCRs, but the quantity of contamination varied, and only PCRs 1, 8, 12 and 15 displayed no detectable PP contamination. Wavenumbers 1490, 1398, 1213, 1195, 1082, 854, 825 and 777 $cm^{-1}$ correspond to the antioxidant Irgafos 168 (Tris(2,4-di-tert-butylphenyl)phosphite) (Badri and Redwan, 2014). which appears to have been added to PCRs 11 and 14 since they display peaks at all these wavenumbers. Trace amounts of PET were identified in some of the

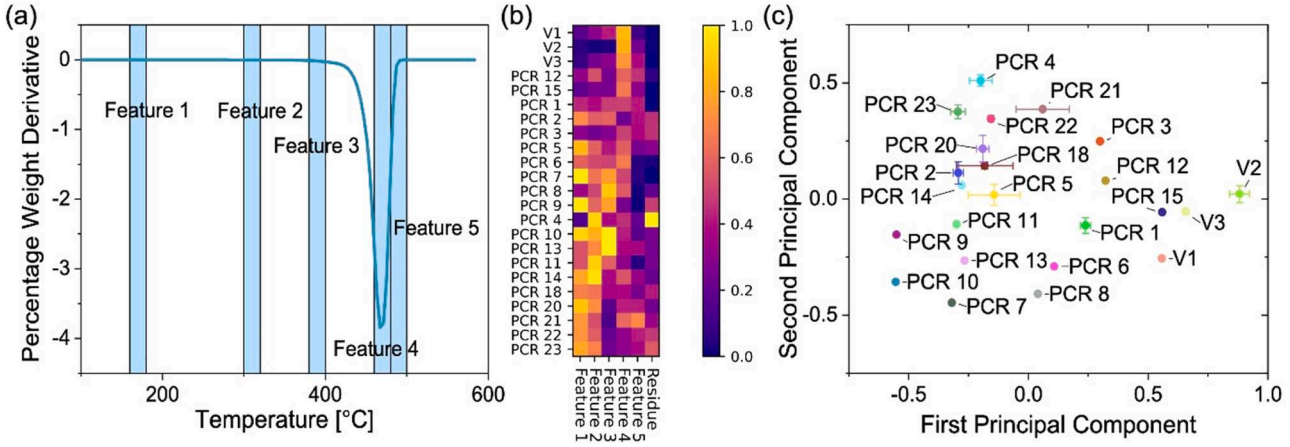


**Fig. 3.** Extracting additional insight from the TGA analysis of the sample set. a) Five of the features extracted from the TGA experimental data. b) Heat map of the features extracted. c) The corresponding PCA for TGA.

PCRs, most notably in PCRs 10 and 13, identified at 1409 and 1018 $cm^{-1}$ (Noda et al., 2007). Additionally, as reported by other researchers, we also identified a peak at 875 $cm^{-1}$ in some resins which we assigned to $CaCO_3$ (Gall et al., 2021). a common filler used in polyolefins (Bartczak et al., 1999). PCR 8 was identified to be contaminated with polyamide due to the assignment of wavenumbers 3297, 1645 and 1541 $cm^{-1}$, (Noda et al., 2007). while PCRs 5, 6, 7 and 9 were identified to contain calcium stearate due to the assignment of wavenumbers 1577 and 1541 $cm^{-1}$ (Gönen et al., 2010). Calcium stearate is added as a lubricant to reduce shear-induced chain scission during processing (Lutz, 1989). The peak at 908 $cm^{-1}$ was assigned to the vinyl functional group, which may give an indication for the catalysis process used to manufacture the resin or be a sign of degradation in PCRs (Gall et al., 2021). The identification of so many different minority components between the resins is further evidence of the heterogeneity and variability that exists in PCR. While clearly additives such as antioxidants and lubricants have been intentionally added, the broad range of contaminants are likely associated with different waste streams and sorting processes (Mager et al., 2023). As it was not possible to obtain information on the plastics source and sorting methods for all PCR suppliers, we cannot make any conclusive correlation to contaminant types. However, specific contaminants may give insights into collection and sorting practices, for example the identification of PET within HDPE would reveal that missorted items, such as PE-laminated PET trays, have entered the HDPE stream after sorting with automated near IR sorting technologies. Later in the paper we will discuss whether the differences in additives and contaminants influence any of the other properties of the PCRs.

Applying PCA to this set of features allows us to visualise and identify the key distinguishing features of the FTIR data (Fig. 2d and e). The first PC is primarily contributed to by peaks due to PP, and so typically the further to the right a resin lies in Fig. 2d and e the greater the PP contamination. The second PC is contributed to by features that are assigned to Irgafos 168, and so we see that this PC separates PCRs 11 and 14 from the other resins (Fig. 2d). The third PC captures the presence of calcium stearate, and so PCRs 5, 7 and 9 sit towards the top of Fig. 2e. The cleanest resins (those with few peaks due to contaminates and additives) lie in the bottom-left corner of Fig. 2e and include all the virgin HDPEs and some PCRs.

### 4.2. *Generating features from all analysis methods*

For the other five techniques, the features were identified in a similar manner to the approach used for the FTIR, often by looking at the derivative of a curve or by extracting a common chemical property from the data. For DSC, features included the width of the primary crystallisation and melt peaks at half the maximum magnitude, as well as the strength of any secondary melt corresponding to polypropylene contaminate (see supplementary information Fig. S4 and Table S5). For tensile testing, the tensile properties extracted were the Young's modulus, ultimate tensile strength, and the strain at break. The strain hardening modulus was also obtained and included in this subset of features. For TGA, along with the residue, the features were defined by the mean derivative in 20 °C intervals. For rheology, the features were the complex viscosity taken at a sample of angular frequencies, the crossover point, and a feature that quantifies how much the curve deviates from linearity (see supplementary information Figs. S6 and S7 and Table S8). Finally, for colour, the L*, a* and b* values were extracted (see supplementary information Fig. S9). We have already looked in detail at the FTIR data, and in the next two sections we will take a deeper dive into the TGA and mechanical testing data. Sections containing more details on the remaining three techniques not covered in detail in this paper can be found in the supplementary information.

## 5. Thermogravimetric analysis exemplar

Conventional interpretation of TGA data focuses on onset temperature and percentage residue mass. Yet, particularly for onset temperature, the data for all samples was very similar to each other (Fig. S10). Each resin is predominantly HDPE and so the vast majority of the thermal decomposition occurred between 460 °C and 480 °C, the temperature range at which HDPE decomposes (Camacho and Karlsson, 2002b; Cuadri and Martín-Alfonso, 2017; Nguyen et al., 2022). Therefore, to distinguish resins, we looked more closely at additional regions of the TGA curve; five of the features extracted from the TGA data were the mean derivatives across 20 °C intervals (160 °C - 180 °C, 300 °C - 320 °C, 380 °C - 400 °C, 460 °C - 480 °C, 480 °C - 500 °C) (see Fig. 3a). Each of these five features was capturing the rate of decomposition of the material within the corresponding temperature range. Additionally, we measured the percentage residue as a feature, which gives an indication of the presence of inorganic fillers and contaminates. The relative values of these features between the PCR samples are shown in Fig. 3b, revealing considerable variability.

By applying PCA to these features, we can visualise how the data obtained from TGA is able to separate the resins. The details of this can be seen in Fig. 3c. The first PC is principally contributed to by Features 1 and 2 which are linked to the volatiles present in the resins. Resins further to the right in the plot have fewer volatiles and so are likely to be less contaminated. They consist of all virgin samples and PCRs 1, 3, 12 and 15. These are the same PCRs that sit with the virgin resins in the bottom-left corner of Fig. 2e in the PCA of the FTIR data. The second PC is contributed to by the residue mass and Feature 3. Feature 3 covers the temperature range 380 °C - 400 °C which captures the start of the main

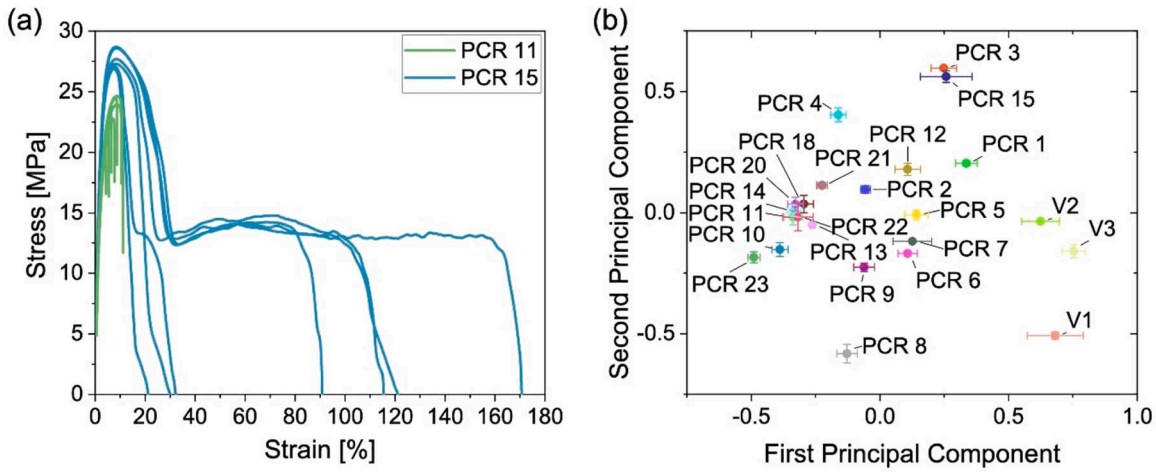


**Fig. 4.** Mechanical testing to differentiate the different PCRs. a) Strain-stress curves produced by tensile testing for 7 repeats of PCRs 11 and 15. b) The first PCs of the features coming from the mechanical tests. The first PC is primarily contributed to by the strain at break, with resins to the right of the plot having a high strain at break. The second PC is primarily contributed to by the SHM, with resins to the bottom of the plot having a higher SHM.

degradation stage of the resins. PCRs 10 and 13 have the highest values for this feature which may be because of the trace amounts of PET in these resins, identified by FTIR, as PET is known to cause an earlier degradation of HDPE (Singh et al., 2020). Although PP is known to have a lower onset temperature for degradation compared to HDPE (Camacho and Karlsson, 2002b; Gall et al., 2021). the resins with high PP contamination (PCRs 18, 20, 21, 22, 23) did not possess a high value for Feature 3 since the presence of HDPE delays the degradation process for PP (Singh et al., 2020). Therefore, the PCA from the TGA provided a combined overview about the volatile contamination, polymer contamination and the presence of any fillers in the PCRs; resins with a high residue are towards the top of the plot, resins towards the bottom of the plot begin the main degradation stage earlier or have low residue, and resins to the right of the plot have less volatile contamination.

## 6. Mechanical testing exemplar

Unlike the subtle differences identified through the features selected for FTIR and TGA, the mechanical testing we carried out showed considerable variation, both between specimens of the same sample and between different PCRs. We used both tensile testing and strain hardening modulus (SHM) measurements to provide quantitative information on the properties of the PCRs. As shown in Fig. 4a, the tensile test results were noticeably different, with all the repeats for PCR 11 breaking at strains of 12% or less, compared to the repeats of PCR 15 where the samples displayed yield and necking behaviour and typically

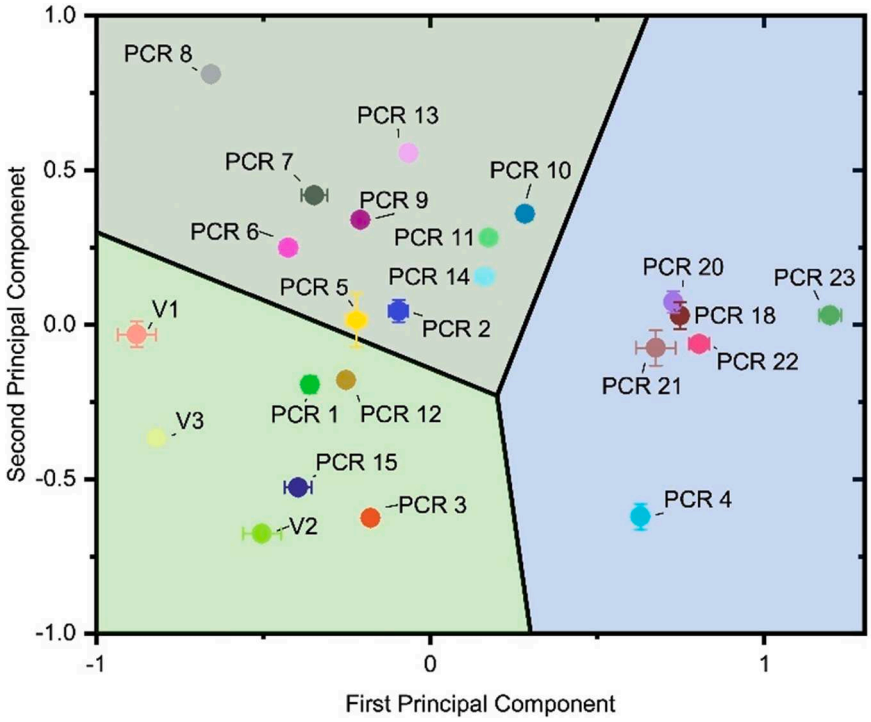


**Fig. 5.** The summary output where the resins are plotted against the first two PCs of the final PCA. The samples are split into 3 clusters using k-means clustering with $k = 3$. The first PC explains 40% of the variation and is primarily contributed to by features linked with PP contamination, and so resins with high PP contamination lie to the right of the plot. The second PC explains 19% of the variation and is primarily contributed to by tensile, rheological and TGA features.

reached strains of at least 75% before breaking.

With tensile testing, we extracted the conventional features from the strain-stress curves, namely Young's modulus, ultimate tensile strength, and the strain at break. As with all features, these values vary between repeats, and so we took the value of each feature to be the mean over the repeats (the plot of the PCA in Fig. 4b displays error bars which indicate the variability in the results). The tensile properties of plastics are typically used as an approach to benchmark different samples and may be predictive of some properties when formed into bottles (McLauchlin et al., 2023). Measurements of the SHM have previously been shown to be an effective way of predicting the environmental stress cracking resistance of virgin HDPE (Cheng et al., 2011; Kurelec et al., 2005). This is an important parameter because the environmental stress cracking resistance of HDPE that has undergone additional extrusion cycles (Zahavich et al., 1997). and direct measurements on HDPE PC (McLauchlin et al., 2023). have been shown to be worse than virgin HDPE. Therefore, combining both the tensile testing data and SHM made up the features of our mechanical tests. The first two PCs of the PCA of these features can be seen in Fig. 4b. The first principal component is primarily contributed to by the strain at break, with resins to the right of the plot having a high strain at break, which were the three virgin samples. The second principal component is primarily contributed to by the SHM, with resins to the bottom of the plot having a higher SHM. Therefore, we would expect resins in the bottom-right of the plot to be the best performing. Those samples with the most favourable combination of properties were the virgin HDPE samples. For PCR resins, there are some that perform well in one or the other, but none that are a match for virgin in both features, showing the gap in quality that exists for HDPE PCR. The mean values of the mechanical testing data can be seen in Table S11 in the SI.

### 7. *Summary analysis of the feature dataset*

As discussed in the methods section, the 56 features obtained by the combined analysis methods were reduced to a 12-dimensional dataset (two dimensions for each of the six analysis techniques) by using PCA. To make a final summary output that allowed the key differences between samples to be visualised, we then applied a second round of PCA to this 12-dimensional dataset. This overall summary output can be seen in Fig. 5. The location of each resin in this PCA space is explained by values of certain features and reveals similarities and differences between the samples. For example, the first principal component, which explains 40 percent of the variation, is primarily contributed to by features that quantify PP contamination, and so resins found on the right-hand side of the plot have high PP contamination. The second principal component, which explains 19 percent of the variation, is contributed to by mechanical, rheological, and TGA features. Most of the resins in the green top-left region appear in this location due to having high values of volatiles identified by the TGA. The key reason PCRs 8 and 4 separate themselves from the other resins is due to their high and low viscosities, respectively. It is unclear why PCR 8 possessed a higher viscosity: this resin also displayed a polyamide contamination that was identified using FTIR, however studies on blending HDPE and polyamide have shown that the blend is less viscous, so this contamination is not the cause of the higher viscosity (Xiang et al., 2012). For this summary analysis we have weighted all features equally. In future work, we will compare our dataset to the performance of the PCRs within packaging applications to identify weighting factors between the PCs. Based on the summary comparison, we suggest that PCRs close to virgin samples (i.e. in the bottom-left region) are most likely to be suitable replacements for virgin resins, whilst resins comparatively far away in the other two regions are likely to not be good substitutes for virgin resins. When selecting a new resin for an application, we could remove risk from the selection process by observing where it sits in this PCA space in comparison to the virgin samples (and other PCRs).

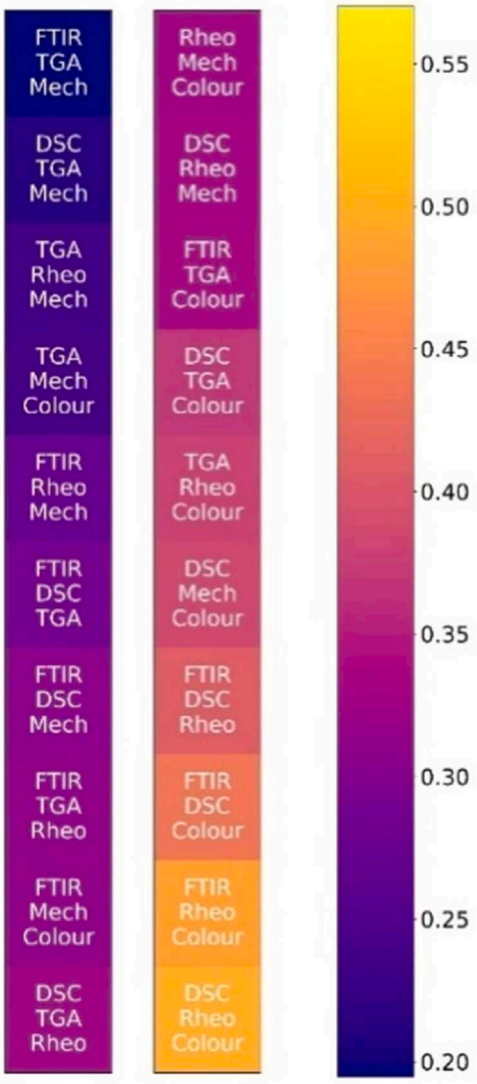


**Fig. 6.** Triplets of experimental techniques that most resemble the whole dataset. Each square represents a triplet of techniques. The darker the square (the lower the value), the more accurately the triplet of techniques distinguishes the resins when compared with the whole dataset. This suggests that, if we had to restrict to just three techniques, the triplet of FTIR, TGA and mechanical techniques would be optimal.

### 8. *Identifying techniques to enable rapid and low-cost classification of PCR*

The experimental data that we have collected from the HDPE PCRs has required using six different characterisation techniques on each resin. While the large number of features extracted from this data can be used to give a picture of how the resins compare with each other, it is also time-consuming and costly. Additionally, not all these methods are typically available for packaging producers. Therefore, we aimed to identify the best subset of three techniques that would still yield an effective classification of the PCRs. A key criterion for classifying PCRs is their similarity to virgin HDPE. To do this, we calculated the mean distance of a given PCR to the virgin resins in the 2D PCA space created using the entire feature dataset (Fig. 5)., and we let this distance be the ground truth distance of the resin to virgin HDPE. Then, for each possible triplet of experiments, we obtain a new 2D PCA space using just the features of the selected triplet of experiments, and computed the mean distance to the virgin resins of a given PCR in this new space. By calculating the difference of this distance to the ground truth, we obtain

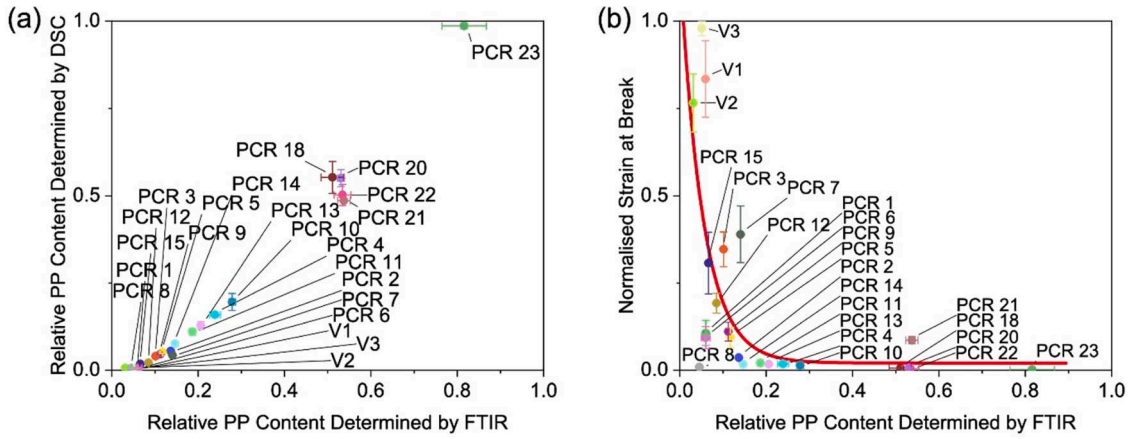


**Fig. 7.** Detecting PP in the PCRs and the effect of PP content on strain at break. a) The normalised feature values of the two methods of quantifying the amount of PP present in the resins. Each point lies close to the diagonal, showing that the two methods strongly agree with each other. We believe that the slight scattering away from the diagonal of PCRs 18, 20, 21 and 22 is due to both noise and inherent variability within the resins. b) The normalised PP content obtained via FTIR plotted against the normalised strain at break. This plot shows that any resin with a normalised PP content value of 0.2 or more has an extremely low strain at break (in practise, the resins are very brittle and break almost immediately). The fitted line is a negative exponential, suggesting that even small contamination of HDPE resins with PP will have a significant impact on performance properties such as the strain at break.

an indication of the information loss resulting from the restriction to these three techniques for this PCR. Taking the mean of the differences over all PCRs in our sample set gives us a total difference, and the triplet with the minimum total difference is identified as the most informative triplet of experiments. The results of this process are shown in Fig. 6, which shows that FTIR, TGA and mechanical data are the triplet of techniques that provide the most effective comparison of the PCRs to virgin; a value of 0.19 was determined as the distance between the complete characterisation data set and the triple of techniques. For context, this value of 0.19 was 18% of the mean distance from virgin for all PCRs in the ground truth. For comparison, the worst performing triplet of techniques (DSC, rheology, and colour measurement) had a value of 0.50 representing a 45% difference from the mean distance from virgin for all PCRs in the ground truth. Different characterisation methods can often provide similar data on the PCR samples, for example the PP content can be indicated by both FTIR and DSC (discussed in more detail later, see Fig. 7). Therefore, these techniques are somewhat interchangeable in terms of differentiating the PCRs. Ultimately, this analysis reveals that the well-informed selection of characterisation methods could be used to select PCR samples with quality approaching that of virgin HDPE.

## 7. Coupling the mechanical data to other features of the dataset

Tensile testing is time-consuming as the resin needs to be processed into specimens which then need to be individually tested, and typically 5–8 specimens are analysed for each sample. Therefore, identifying approaches that can predict the mechanical properties will have significant value in terms of accelerating the selection of appropriate PCR samples.

One of the major factors that has been shown to have a significant detrimental effect on the mechanical properties of HDPE is contamination with PP (Demets et al., 2022). For example, Karaagac et al. have shown that, by systematically blending recycled PP contamination into HDPE PCR, the elongation at break reduced with increased PP content (Karaagac et al., 2021b). Our analysis has shown that both DSC and FTIR were effective at identifying the presence of PP in HDPE samples. For DSC, a melting point at ~160 °C was observed as a secondary peak in the melt curve. Identifying the strength of this peak gives us an indication as to the amount of PP contamination present in the resin. For FTIR, PP has several characteristic peaks as previously discussed. We focus on just one such peak at a wavenumber of 972 $cm^{-1}$ that lies in a section of the spectrum where there were no other peaks present. By taking the integral of the spectrum in the interval from 980 to 965 $cm^{-1}$, the outputted value again gives an indication as to the presence of PP contamination in the resins. By comparing these two methods, it was possible to see a good agreement between the methods in capturing the comparative PP content present in the resins, as shown in Fig. 7a. While the FTIR method was more sensitive, it was always possible to detect PP when present using both methods. We used the FTIR method to compare the amount of PP in the PCRs with the tensile testing data, which showed that samples with increased PP content experienced a significant reduction in the strain at break (Fig. 7b). The relationship identified could be fitted with a negative exponential, suggesting that even small contamination of HDPE resins with PP had a significant impact on performance properties such as the strain at break. Our dataset confirms the prior literature finding regarding PP contamination in HDPE being highly detrimental (Demets et al., 2022; Karaagac et al., 2021b). and additionally we show that this relationship holds true for commercial PCRs where the PP is an unintended contaminant. This is significant because it provides an approach to rapidly identifying problematic resins with high PP content purely by FTIR analysis.

## 8. Conclusion

To conclude, we have curated a sample set of 23 HDPE resins (3 virgin, 20 PCR) and have performed extensive characterisation of the resins to produce a feature-rich dataset. The feature extraction process has combined traditional methods with novel approaches that have identified new features within the data to enable the differentiation of similar materials. Analysis of this feature dataset gives an indication of how resins compare with each other, and crucially how PCRs compare with virgin HDPEs. Relationships can be identified, such as the impact of PP content on the strain at break. Improving our understanding of the general differences between PCRs and virgin HDPE, and how these differences impact performance, can inform the current approaches to improving the properties of PCRs for specific applications. Our feature dataset can be probed further to reveal important structure-property relationships, which will be reported in future papers. While the extensive characterisation that we have performed may not be practical for typical packaging producers, we have identified a reduced set of techniques that enables a good characterisation of a resin with minimal data loss. As a result, fair comparisons with other resins can be made without performing the full set of characterisation methods. The potential for new resins to be run through the method of analysis exhibited should enable a comparison of the new resin with the large dataset of

resins already curated. We believe that this can help to de-risk the selection process when considering replacing virgin plastics with PCRs in terms of mechanical and physical properties for a given application, allowing both an increase in PCR use, and an improvement in the quality of the PCRs being offered.

## CRediT authorship contribution statement

**Philip Smith:** Writing – review & editing, Writing – original draft, Visualization, Methodology, Formal analysis, Data curation. **Andy McLauchlin:** Writing – review & editing, Writing – original draft, Methodology, Formal analysis, Data curation, Investigation. **Tom Franklin:** Writing – review & editing, Formal analysis. **Peiyao Yan:** Writing – review & editing, Methodology, Formal analysis. **Emily Cunliffe:** Writing – review & editing, Formal analysis. **Tom Hasell:** Writing – review & editing, Supervision, Funding acquisition. **Vitaliy Kurlin:** Supervision, Funding acquisition. **Colin Kerr:** Writing – review & editing, Resources. **Jonathan Attwood:** Writing – review & editing, Resources, Methodology. **Michael P. Shaver:** Writing – review & editing, Visualization, Supervision, Project administration, Methodology, Funding acquisition, Data curation, Conceptualization. **Tom O. McDonald:** Writing – review & editing, Visualization, Supervision, Project administration, Methodology, Funding acquisition, Data curation, Conceptualization.

## Declaration of competing interest

The authors declare the following financial interests/personal relationships which may be considered as potential competing interests:

Unilever and IPL Brightgreen provided samples, analysis and expertise to this project as part of their efforts to improve the sustainability in the packaging sector. Kerr is an employee of Unilever and Attwood is an employee of IPL Brightgreen. For the other authors, they have all worked on this collaborative project with Unilever and IPL Brightgreen. Additionally, McDonald, Kurlin and Shaver have previously received financial support or in-kind support for prior research projects with Unilever.

## Data availability

Data will be made available on request.

## Acknowledgements

We are incredibly grateful for the funding provided for this project by the UKRI's Enabling Research competition in the Smart Sustainable Plastic Packaging (SSPP) challenge, grant number NE/V010778/1 and NE/V010778/2. This work was also supported by the Henry Royce Institute for Advanced Materials, funded through EPSRC grants EP/R00661X/1, EP/S019367/1, EP/P025021/1, EP/P025498/1 and the Sustainable Materials Innovation Hub, funded through the European Regional Development Fund OC15R19P.

## Supplementary materials

Supplementary material associated with this article can be found, in the online version, at doi:10.1016/j.resconrec.2024.107538.

## References

Abejón, R., Bala, A., Vázquez-Rowe, I., Aldaco, R., Fullana-i-Palmer, P., 2020. When plastic packaging should be preferred: life cycle analysis of packages for fruit and vegetable distribution in the Spanish peninsular market. Resour. Conserv. Recycl. 155, 104666 https://doi.org/10.1016/j.resconrec.2019.104666.

Achilias, D.S., 2022. Thermal Analysis in Polymer Recycling. Thermal Analysis of Polymeric Materials. Wiley, pp. 485–508. https://doi.org/10.1002/9783527828692.ch14.

Akhras, M.H., Freudenthaler, P.J., Straka, K., Fischer, J., 2023. From bottle caps to frisbee—a case study on mechanical recycling of plastic waste towards a circular economy. Polym. (Basel) 15, 2685. https://doi.org/10.3390/polym15122685.

Alzerreca, M., Paris, M., Boyron, O., Orditz, D., Louarn, G., Correc, O., 2015. Mechanical properties and molecular structures of virgin and recycled HDPE polymers used in gravity sewer systems. Polym. Test. 46, 1–8. https://doi.org/10.1016/j.polymertesting.2015.06.012.

ASTM International, 2012. Standard Test Method for Transition Temperatures and Enthalpies of Fusion and Crystallization of Polymers by Differential Scanning. ASTM Stand. https://doi.org/10.1520/D3418-15.

Bachmann, M., Zibunas, C., Hartmann, J., Tulus, V., Suh, S., Guillén-Gosálbez, G., Bardow, A., 2023. Towards circular plastics within planetary boundaries. Nat. Sustain. 6, 599–610. https://doi.org/10.1038/s41893-022-01054-9.

Badri, K.H., Redwan, A., 2014. Fire-Resist Bio-Based Polyurethane for Structural Foam Application, in: physical Chemistry of Macromolecules. Apple Academic Press, pp. 237–348. https://doi.org/10.1201/b16706-17.

Bartczak, Z., Argon, A., Cohen, R., Weinberg, M., 1999. Toughness mechanism in semi-crystalline polymer blends: II. High-density polyethylene toughened with calcium carbonate filler particles. Polym. (Guildf) 40, 2347–2365. https://doi.org/10.1016/S0032-3861(98)00444-3.

Benyathiar, P., Kumar, P., Carpenter, G., Brace, J., Mishra, D.K., 2022. Polyethylene terephthalate (PET) bottle-to-bottle recycling for the beverage industry: a review. Polym. (Basel) 14, 2366. https://doi.org/10.3390/polym14122366.

Camacho, W., Karlsson, S., 2002a. Simultaneous determination of molecular weight and crystallinity of recycled HDPE by infrared spectroscopy and multivariate calibration. J. Appl. Polym. Sci. 85, 321–327. https://doi.org/10.1002/app.10634.

Camacho, W., Karlsson, S., 2002b. Assessment of thermal and thermo-oxidative stability of multi-extruded recycled PP, HDPE and a blend thereof. Polym. Degrad. Stab. 78, 385–391. https://doi.org/10.1016/S0141-3910(02)00192-1.

Camacho, W., Karlsson, S., 2001. NIR, DSC, and FTIR as quantitative methods for compositional analysis of blends of polymers obtained from recycled mixed plastic waste. Polym. Eng. Sci. 41, 1626–1635. https://doi.org/10.1002/pen.10860.

Campanale, C., Savino, I., Massarelli, C., Uricchio, V.F., 2023. Fourier transform infrared spectroscopy to assess the degree of alteration of artificially aged and environmentally weathered microplastics. Polym. (Basel) 15, 911. https://doi.org/10.3390/polym15040911.

Cheng, J.J., Polak, M.A., Penlidis, A., 2011. Influence of micromolecular structure on environmental stress cracking resistance of high density polyethylene. Tunn. Undergr. Sp. Technol. 26, 582–593. https://doi.org/10.1016/j.tust.2011.02.003.

Cuadri, A.A., Martín-Alfonso, J.E., 2017. The effect of thermal and thermo-oxidative degradation conditions on rheological, chemical and thermal properties of HDPE. Polym. Degrad. Stab. 141, 11–18. https://doi.org/10.1016/j.polymdegradstab.2017.05.005.

da Silva, D.J., Wiebeck, H., 2022. ATR-FTIR spectroscopy combined with chemometric methods for the classification of polyethylene residues containing different contaminants. J. Polym. Environ. 30, 3031–3044. https://doi.org/10.1007/s10924-022-02396-3.

Demets, R., Grodent, M., Van Kets, K., De Meester, S., Ragaert, K., 2022. Macromolecular insights into the altered mechanical deformation mechanisms of non-polyolefin contaminated polyolefins. Polym. (Basel) 14, 239. https://doi.org/10.3390/polym14020239.

Demets, R., Van Kets, K., Huysveld, S., Dewulf, J., De Meester, S., Ragaert, K., 2021. Addressing the complex challenge of understanding and quantifying substitutability for recycled plastics. Resour. Conserv. Recycl. 174, 105826 https://doi.org/10.1016/j.resconrec.2021.105826.

Freudenthaler, P.J., Fischer, J., Liu, Y., Lang, R.W., 2022. Short-and long-term performance of pipe compounds containing polyethylene post-consumer recyclates from packaging waste. Polym. (Basel) 14. https://doi.org/10.3390/polym14081581.

Gall, M., Freudenthaler, P.J., Fischer, J., Lang, R.W., 2021. Characterization of composition and structure–property relationships of commercial post-consumer polyethylene and polypropylene recyclates. Polym. (Basel) 13. https://doi.org/10.3390/polym13101574.

Gönen, M., Öztürk, S., Balköse, D., Okur, S., Ülkü, S., 2010. Preparation and characterization of calcium stearate powders and films prepared by precipitation and Langmuir−Blodgett techniques. Ind. Eng. Chem. Res. 49, 1732–1736. https://doi.org/10.1021/ie901437d.

Hahladakis, J.N., Purnell, P., Iacovidou, E., Velis, C.A., Atseyinku, M., 2018. Post-consumer plastic packaging waste in England: assessing the yield of multiple collection-recycling schemes. Waste Manag. 75, 149–159. https://doi.org/10.1016/j.wasman.2018.02.009.

ISO, 2016. ISO 17855-2: Plastics — Polyethylene (PE) Moulding and Extrusion Materials — Part 2: Preparation of Test Specimens and Determination of Properties.

ISO, 2015. ISO 18488:2015 Polyethylene (PE) Materials For Piping Systems Determination of Strain Hardening Modulus in Relation to Slow Crack Growth.

ISO, 2012. ISO527 Determination of Tensile Properties.

Karaagac, E., Jones, M.P., Koch, T., Archodoulaki, V.M., 2021a. Polypropylene contamination in post-consumer polyolefin waste: characterisation, consequences and compatibilisation. Polym. (Basel) 13, 2618. https://doi.org/10.3390/polym13162618.

Karaagac, E., Koch, T., Archodoulaki, V.-M.M., 2021b. The effect of PP contamination in recycled high-density polyethylene (rPE-HD) from post-consumer bottle waste and their compatibilization with olefin block copolymer (OBC). Waste Manag. 119, 285–294. https://doi.org/10.1016/j.wasman.2020.10.011.

Kurelec, L., Teeuwen, M., Schoffeleers, H., Deblieck, R., 2005. Strain hardening modulus as a measure of environmental stress crack resistance of high density polyethylene. Polym. (Guildf.) 46, 6369–6379. https://doi.org/10.1016/j.polymer.2005.05.061.

Lisiecki, M., Damgaard, A., Ragaert, K., Astrup, T.F., 2023. Circular economy initiatives are no guarantee for increased plastic circularity: a framework for the systematic comparison of initiatives. Resour. Conserv. Recycl. 197, 107072 https://doi.org/10.1016/j.resconrec.2023.107072.

Lutz, J.T. (Ed.), 1989. Thermoplastic Polymer additives: Theory & Practice. M. Dekker, New York.

Mager, M., Berghofer, M., Fischer, J., 2023. Polyolefin recyclates for rigid packaging applications: the influence of input stream composition on recyclate quality. Polym. (Basel) 15, 2776. https://doi.org/10.3390/polym15132776.

Manivannan, A., Seehra, M.S., 1997. Identification and quantification of polymers in waste plastics using differential scanning calorimetry. ACS Div. Fuel Chem. Prepr. 42, 1028–1030.

McIlgorm, A., Raubenheimer, K., McIlgorm, D.E., Nichols, R., 2022. The cost of marine litter damage to the global marine economy: insights from the Asia-Pacific into prevention and the cost of inaction. Mar. Pollut. Bull. 174, 113167 https://doi.org/10.1016/j.marpolbul.2021.113167.

McLauchlin, A.R., Hall, D., Feldman, D., Anderson, P., Newman, M., Hasell, T., McDonald, T.O., 2023. Improving the performance of post-consumer resin feedstocks for rigid packaging applications: a pilot-scale assessment. Resour. Conserv. Recycl. 199, 107209 https://doi.org/10.1016/j.resconrec.2023.107209.

Nguyen, K.Q., Cousin, P., Mohamed, K., Robert, M., Benmokrane, B., 2022. Comparing short-term performance of corrugated HDPE pipe made with or without recycled resins for transportation infrastructure applications. J. Mater. Civ. Eng. 34, 1–9. https://doi.org/10.1061/(asce)mt.1943-5533.0004067.

Noda, I., Dowrey, A.E., Haynes, J.L., Marcott, C., 2007. Group Frequency Assignments For Major Infrared Bands Observed in Common Synthetic Polymers, in: Physical Properties of Polymers Handbook. Springer, New York, New York, NY, pp. 395–406. https://doi.org/10.1007/978-0-387-69002-5_22.

Oblak, P., Gonzalez-Gutierrez, J., Zupančič, B., Aulova, A., Emri, I., 2015. Processability and mechanical properties of extensively recycled high density polyethylene. Polym. Degrad. Stab. 114, 133–145. https://doi.org/10.1016/j.polymdegradstab.2015.01.012.

OECD, 2022. Policy Highlights: Global Plastics Outlook.

Orzan, E., Janewithayapun, R., Gutkin, R., Lo Re, G., Kallio, K., 2021. Thermo-mechanical variability of post-industrial and post-consumer recyclate PC-ABS. Polym. Test. 99, 107216 https://doi.org/10.1016/j.polymertesting.2021.107216.

PlasticEurope: Plastics – The Facts 2022, 2022. Plastics – the facts 2022 [WWW Document]. Plast. Eur. URL https://plasticseurope.org/knowledge-hub/plastics-the-facts-2022/.

Ringnér, M., 2008. What is principal component analysis? Nat. Biotechnol. 26, 303–304. https://doi.org/10.1038/nbt0308-303.

Schyns, Z.O.G., Shaver, M.P., 2020. Mechanical recycling of packaging plastics: a review. Macromol. Rapid Commun. 1–27. https://doi.org/10.1002/marc.202000415, 2000415.

Silva, N., Molina-Besch, K., 2023. Replacing plastic with corrugated cardboard: a carbon footprint analysis of disposable packaging in a B2B global supply chain—a case study. Resour. Conserv. Recycl. 191 https://doi.org/10.1016/j.resconrec.2023.106871.

Singh, R.K., Ruj, B., Sadhukhan, A.K., Gupta, P., 2020. A TG-FTIR investigation on the co-pyrolysis of the waste HDPE, PP, PS and PET under high heating conditions. J. Energy Inst. 93, 1020–1035. https://doi.org/10.1016/j.joei.2019.09.003.

Tamburini, E., Costa, S., Summa, D., Battistella, L., Fano, E.A., Castaldelli, G., 2021. Plastic (PET) vs bioplastic (PLA) or refillable aluminium bottles – What is the most sustainable choice for drinking water? A life-cycle (LCA) analysis. Environ. Res. 196, 110974 https://doi.org/10.1016/j.envres.2021.110974.

Tenhunen-Lunkka, A., Rommens, T., Vanderreydt, I., Mortensen, L., 2023. Greenhouse Gas Emission Reduction Potential of European Union's Circularity Related Targets for Plastics, Circular Economy and Sustainability. Springer International Publishing. https://doi.org/10.1007/s43615-022-00192-8.

Thomson, H., Illingworth, K., McCoach, H., Jefferson, M., Morgan, S., 2018. PlasticFlow 2025: Plastic Packaging Flow Data Report. ENG017-011.

Van Beek, D.J.M., Deblieck, R., 2011. Strain hardening: an elegant and fast method to predict the slow crack growth behavior of HDPE pipe materials. Soc. Plast. Eng. - EUROTEC 2011 Conf. Proc.

Van Belle, A.V., Demets, R., Mys, N., Van Kets, K.V., Dewulf, J., Van Geem, K.V., De Meester, S.D., Ragaert, K., 2020. Microstructural contributions of different polyolefins to the deformation mechanisms of their binary blends. Polym. (Basel) 12, 1–21. https://doi.org/10.3390/POLYM12051171.

Xiang, F., Shi, Y., Li, X., Huang, T., Chen, C., Peng, Y., Wang, Y., 2012. Cocontinuous morphology of immiscible high density polyethylene/polyamide 6 blend induced by multiwalled carbon nanotubes network. Eur. Polym. J. 48, 350–361. https://doi.org/10.1016/j.eurpolymj.2011.11.013.

Zahavich, A.T.P., Latto, B., Takacs, E., Vlachopoulos, J., 1997. The effect of multiple extrusion passes during recycling of high density polyethylene. Adv. Polym. Technol. 16, 11–24. https://doi.org/10.1002/(SICI)1098-2329(199721)16:1<11::AID−ADV2>3.0.CO;2-M.

Zheng, J., Suh, S., 2019. Strategies to reduce the global carbon footprint of plastics. Nat. Clim. Chang. 9, 374–378. https://doi.org/10.1038/s41558-019-0459-z.